

## Effect of $a_0/W$ Ratio on Fracture Toughness Parameter of Extra Deep Drawn Steel Sheets: Experimental and Finite Element Studies

Vikas Chaudhari<sup>a</sup> and D.M. Kulkarni<sup>b</sup>

*Mech. Engg. Dept., BITS-Pilani, Goa Campus, India*

<sup>a</sup>Corresponding Author, Email: [vikas@goa.bits-pilani.ac.in](mailto:vikas@goa.bits-pilani.ac.in)

<sup>b</sup>Email: [mk@goa.bits-pilani.ac.in](mailto:mk@goa.bits-pilani.ac.in)

### ABSTRACT:

Fracture toughness parameter is significantly affected by specimen dimensions i.e. specimen thickness ( $B$ ), width ( $W$ ) and unbroken ligament length ( $W-a_0$ ) in elastic-plastic region. Present study is about the third dimension of test specimen ( $W-a_0$ ). In order to investigate effect of  $a_0/W$  ratio on fracture toughness parameter, fracture test and finite element - cohesive zone model (CZM) simulation tool are used. Fracture tests are carried out on extra deep drawn (EDD) steel sheets using compact tension (CT) type specimens with different  $a_0/W$  ratio (0.5, 0.525, 0.55 and 0.575). After successive experimental attempts, load drop technique is used as a fracture criterion. Critical CTOD is used as a fracture toughness parameter. An alternative constant traction separation law is used to account for maximum load and large load line displacements. Experimental findings as well as finite element studies show that the critical CTOD decreases with  $a_0/W$  ratio. It has been observed that as  $a_0/W$  ratio increases, the location of plastic hinge shifts towards the crack tip (i.e. size of tensile plastic zone reduces), which reduces fracture toughness. That is, the material is less resistant to crack growth for deeper cracks.

### KEYWORDS:

Fracture mechanics;  $a_0/W$  ratio; Critical CTOD; CZM; EDD steel sheets

### CITATION:

V. Chaudhari and D.M. Kulkarni. 2016. Effect of  $a_0/W$  ratio on fracture toughness parameter of extra deep drawn steel sheets: experimental and finite element studies, *Int. J. Vehicle Structures & Systems*, 8(4), 198-203. doi:10.4273/ijvss.8.4.03

### ACRONYMS AND NOMENCLATURE:

CTOD	Crack tip opening displacement
CZM	Cohesive zone model
$a_0$	Initial crack length
$W, B$	Width and thickness of specimen
$\rho$	Notch radius
$J_i$	J-integral at crack initiation
$P_c$	Critical load
$\delta_c$	Critical CTOD
$\sigma_0$	Cohesive strength
$k_P$	Penalty stiffness
$\Gamma_0$	Fracture energy
$\delta_f$	Separation distance

## 1. Introduction

In practice, steel components are too large in dimensions and too expensive to be tested in their operating conditions for the characterization of fracture toughness. Therefore fracture toughness is evaluated by using standard laboratory test procedures recommended by ASTM. The advantage of following standard test procedures is the cost associated with the specimens that can be tested in laboratories is less as well as low load capacity machines can be used for the testing. However the fracture toughness data obtained from standard test procedures is corresponding to plane strain fracture toughness (lower shelf fracture toughness) [1,2]. Under

large scale yielding the specimen boundaries affect the crack tip stress field by relaxing the triaxial stress state. In such situations, fracture toughness is strongly dependent on specimen size and crack depth. The fracture toughness values for shallow cracks are higher than those determined from standard deep cracked test specimens which is referred as the constraint effect [3,4]. Therefore, there is a strong incentive to reduce excess conservatism to provide more realistic estimate of remaining life of the components [5]. For this purpose, the experimental and numerical investigations are required to characterize the constraint quantitatively [2].

Present work aims to investigate effect of  $a_0/W$  ratio on fracture toughness parameter of extra deep drawn (EDD) steel sheets. EDD steel sheets are widely used in industrial applications. EDD steel has superior formability and non-ageing characteristics. These steels are low carbon, Al-killed steels. Exterior components such as car body, starter, end-covers and petrol tanks are made of EDD grade steel sheets. Apart from automobile industries, the EDD steel sheets are extensively used in enamelling applications such as bath sink units, kitchenware, cooker, washing machine and refrigerator bodies.

## 2. Experimental procedure

Earlier research work published by Kulkarni et al [6] and Chaudhari et al [7-10] shows the experimental procedure

involved in the testing of EDD steel sheets using compact tension (CT) type specimens. The dimensions of the CT specimens used in the present work were chosen from the recommended design standard given in American Society for Testing and Materials (ASTM) E1820. Specimens were fabricated by wire electric discharge machine to maintain exact relationship among all the dimensions as per the standards. The configuration of the test specimen is shown in Fig. 1 (Specimen dimensions are  $W = 40\text{mm}$ ,  $B = 2\text{mm}$  and  $\rho = 0.125\text{ mm}$ ). Four specimens of identical size and different  $a_0/W$  ratios (0.5, 0.525, 0.55 and 0.575) were considered for the present study. These specimens were coded as A1, A2, ..., A4. The chemical composition of the investigated EDD steel is given in Table 1.

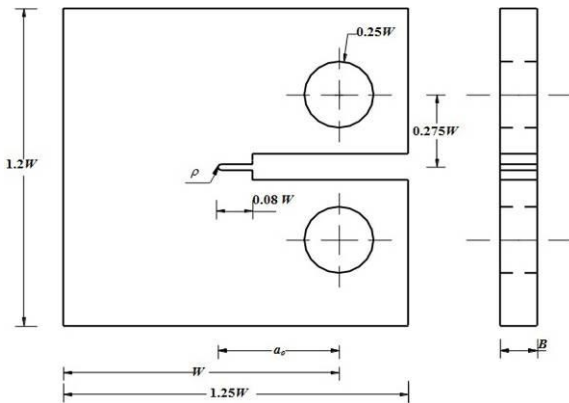


Fig. 1: Dimensions of CT specimen as per ASTM standard

Table 1: Composition of the investigated EDD steel sheet in wt. %

C	Mn	S	P	Si	Al	N	Fe
0.04	0.18	0.007	0.005	0.012	0.044	0.0034	Balance

Fracture tests were carried out at room temperature (300K) using a universal testing machine. All four specimens were tested at 0.2 strain rate. Crack mouth opening displacement (CMOD) gauge was used to measure load-line displacement. Anti-buckling fixtures were used to avoid out-of-plane buckling. The experimental set up is shown in Fig. 2.



Fig. 2: Test set-up for fracture test

During such tests, the magnitude of load ( $P$ ) and load-line displacement ( $V_l$ ) were recorded together with time. The load drop technique [6] was used as a fracture criterion to measure fracture parameters. According to this criterion, the load drops at a particular instant when crack is initiated. This load was considered as a critical load ( $P_c$ ). At that instance of time, the loading of a

specimen was discontinued, and the specimen was taken out for subsequent measurement of crack tip opening displacement ( $CTOD$ ). As the plastic load-line displacement was high in case of EDD steel sheets, crack flank opening angle ( $CFOA$ ) method [8] was used to find plastic  $CTOD$ .

### 3. Finite element analysis

Finite element analysis (FEA) is one of the numerical methods, widely used in fracture mechanics applications. The important aspects of FEA are selection of elements to model the geometry, crack region and modeling of the material behavior. Cohesive zone model (CZM) is widely used to characterize the fracture behavior of the ductile materials. CZM removes the crack tip singularity and represents physics of the fracture process at the atomic scale. In present study, CZM was formulated to verify the critical  $CTOD$  values, measured using  $CFOA$  method.

#### 3.1. Loading and boundary conditions

The loading pins were modeled as rigid pins to avoid any severe local deformation at the contact points. The contact between loading pins and plane stress elements was considered smooth (frictionless). The boundary conditions on the CT specimen model restricted the displacements along x-direction and y-direction and rotation about z-direction of the lower loading pin. The load was applied at upper loading pin using an incremental displacement step along y-direction where as its displacement along x-direction and rotation about z-direction were constrained. The LLD was calculated as the relative nodal displacements at the center of loading pins.

#### 3.2. Cohesive zone model

Two-dimensional CZM was developed for CT type specimen geometry following the design standards, ASTM E1820- 11. This model was used to compare experimental load versus load line displacement (LLD) curves with the elastic-plastic softening response of EDD steel sheets. This model included mesh, boundary conditions, special features such as the cohesive elements on the expected crack path and a nonlinear step definition to solve the nonlinear fracture problem. As shown in Fig. 3.

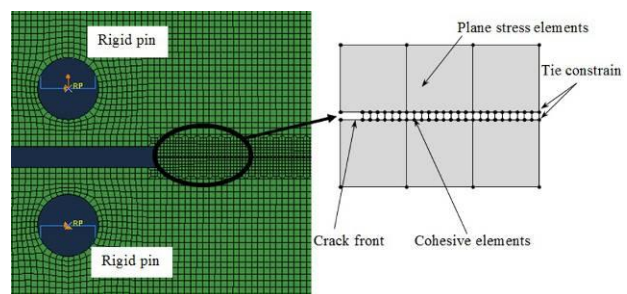


Fig. 3: FE model, bulk elements and cohesive elements

The CT specimen model had a bulk section made with two dimensional plain stress elements defined by its elastic-plastic properties. There were 5582 nodes and 5377 four noded quadrilateral plane stress elements. The crack path was modeled separately using cohesive

elements (COH2D4) defined by a traction–separation law. The cohesive elements were placed along the crack path (402 nodes and 200 cohesive elements). Cohesive elements were taken to be square of side 0.1 mm. Plane stress elements around cohesive zone were taken to be squares of side 0.5 mm. Because the size of cohesive elements was different from the surrounding elements, cohesive elements were placed along the crack path in the model using a tie constraint.

**3.3. Shape of traction-separation curve**

Many variations of cohesive zone models are proposed in literature and successfully applied to predict fracture behaviors. The applications of the CZM mostly fall in the range of exponential [11-14], linear/bilinear [15-20] and trapezoidal [21] forms of traction-separation laws. Fig. 4 shows the representative cohesive law shapes. Among the various forms of cohesive laws, there is one common feature that is the magnitude of the cohesive traction usually increases with accrued separation between the cohesive surfaces, and after a critical peak value is reached, the traction drops towards zero with further separation. For the ductile materials, literature suggests [22-24] use of exponential or constant variation of normal traction with the relative normal displacement.

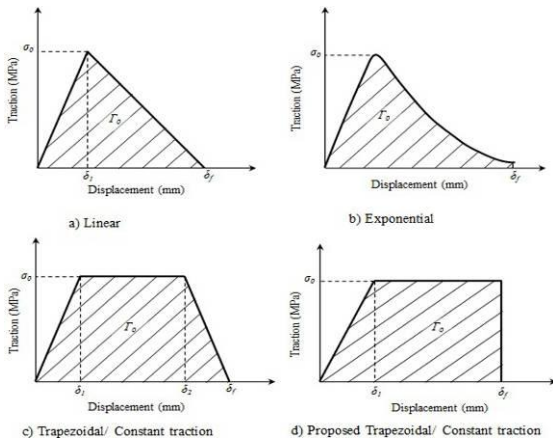


**Fig. 4: Different forms of the traction separation law**

**4. Validation of cohesive zone model**

Specimen A1 was first analyzed. The commonly adopted approach assumes certain law of the traction-separation relation for the cohesive zone [Fig. 4 (a, b, c and d)] and the cohesive parameters are treated as modeling constants. The key cohesive parameters describing the CZM consist of the cohesive strength ( $\sigma_0$ ), defined by the peak value of the traction-separation curve; the cohesive energy ( $\Gamma_0$ ) represented by the area under the traction-separation curve, maximum separation distance ( $\delta_f$ ) and initial cohesive stiffness often called as penalty stiffness ( $k_p$ ). The cohesive parameters cannot be measured in a direct way for ductile materials but have to be identified by fitting finite element results to experimental data [25]. The key features of a CZM include the shape of the traction-separation curve and the value of the cohesive parameters. In the present case, the material used is high ductile material with load maxima as fracture criteria. The constant traction law is chosen with  $\delta_2 = \delta_f$ , that is Fig. 4d. The analysis is done using linear, exponential and proposed constant traction law and results are

compared with the experimental load versus LLD curve (Fig. 5). To validate CZM, maximum value of load and  $J$ -integral based on load versus LLD are considered. To determine  $J$ -integral, the procedure listed in ASTM E1820-11 is used.

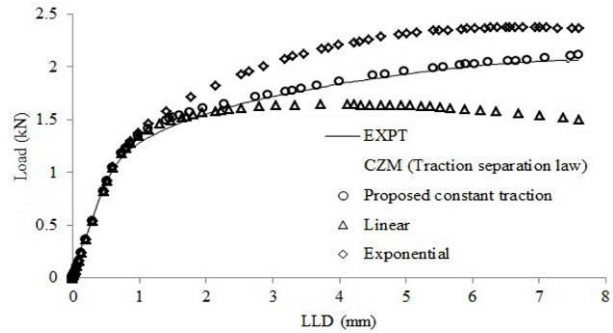


**Fig. 5: Comparison of load-LLD curves based on three cohesive laws with experimental data (Specimen code A1,  $a_0/W = 0.5$ )**

From Fig. 5 it is observed that linear traction separation law i.e. Fig. 4(a) under estimates the maximum load and it is suitable for brittle material/linear elastic analysis [16-19]. Exponential law (Fig. 4 b) is used for ductile materials; however in the present case it under estimates load line displacement. For instance, experimentally, the maximum value of load appears corresponding to 7.59mm LLD whereas using exponential law, maximum value of load appears corresponding to 6.63mm LLD. Similar observation is found by using constant traction separation law i.e. Fig. 4 (c). As load values obtained by using exponential law and constant traction separation law (Fig. 4 (b&c)) are almost same, only results corresponding to exponential law are shown in Fig. 5. The results from proposed constant traction separation law (Fig. 4 d) are found to be close to the experimental observations; the maximum load is over-estimated only by 2.3% and corresponding  $J$ -integral value at crack initiation i.e.  $J_i$ , based on load vs LLD is 1.84% more than experimental value.

Thus the proposed constant traction- separation law is considered for the further study. To determine cohesive strength, number of trials had been performed by choosing different values of cohesive strength and the results are compared with the experimental observations. For demonstration purpose three different values of cohesive strength, 1)  $\sigma_0 = 180$  MPa (i.e.  $\sigma_0 = \sigma_y$ ), 2)  $\sigma_0 = 270$  MPa and 3)  $\sigma_0 = 460$  MPa (i.e.  $\sigma_0 = \sigma_{UTS}$ ) are considered (Fig. 6).

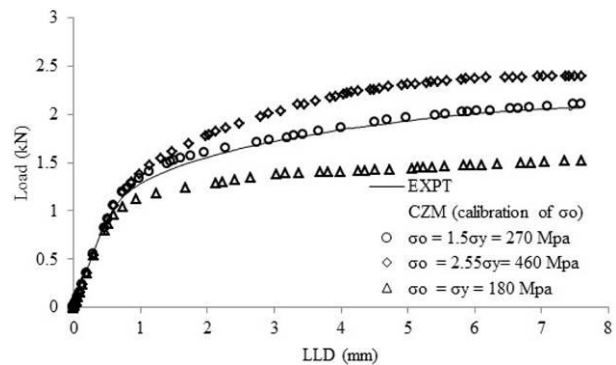


**Fig. 6: Effect of cohesive strength ( $\sigma_0$ ) on load-LLD curve (Specimen code A1,  $a_0/W = 0.5$ )**

It is observed that, higher value of cohesive strength overestimates the load whereas lower value of cohesive strength, underestimates the load. The moderate value of cohesive strength gives the load values close to the experimental results. For the present case, the cohesive strength for CZM is taken as 270 MPa. The remaining specimens i.e. A2–A4 were studied using proposed constant traction separation law. The calibrated cohesive parameters for all the tested specimens (A1-A4) are given in Table 2. The percentage difference between peak load from experimental data and peak load calculated from CZM is found to be within 3.18% (Table 3), thus the values of peak loads calculated from CZM are acceptable. The percentage difference between  $J_i$  from experimental data and  $J_i$  calculated from CZM for all cases is found to be within 3.30% (Table 4), thus the values of  $J_i$  calculated from CZM are acceptable.

**Table 2: Calibrated cohesive parameters (Specimen A1 - A4)**

Specimen Code	$a_o/W$ ratio	Cohesive Stiffness $k_p$ (N/mm <sup>3</sup> )	Cohesive strength $\sigma_0$ (MPa)	Cohesive Energy $\Gamma_0$ (N/mm)
A1	0.5	1500	270	708.02
A2	0.525	1500	290	716.39
A3	0.55	3000	300	646.00
A4	0.575	3000	300	623.03

**Table 3: Comparison of peak load values (Specimen A1 – A4)**

Specimen	$a_o/W$	Peak load, (Expt)	Peak load, (CZM)	% difference
A1	0.5	2.07	2.12	2.30
A2	0.525	1.98	2.02	2.17
A3	0.55	1.78	1.84	3.18
A4	0.575	1.62	1.64	1.28

**Table 4: Comparison of  $J_i$  values (Specimen A1 - A4)**

Specimen code	A1	A2	A3	A4
$a_o/W$ ratio	0.5	0.525	0.55	0.575
J-integral, kJ/m <sup>2</sup> (Expt)	661.82	652.08	623.26	613.22
J-integral, kJ/m <sup>2</sup> (CZM)	674.02	669.02	643.83	616.77
% difference	1.84	2.6	3.3	0.58

### 5. Results and discussions

It is observed from Table 3 that the critical load decreases with increasing values of  $a_o/W$  ratio. It is expected, because as  $a_o/W$  ratio increases, plate stiffness reduces which further reduces the critical load. The results on critical CTOD for different  $a_o/W$  ratios are presented in Fig. 7. It shows the variation of critical CTOD with  $a_o/W$  ratio (0.5 - 0.575). From Fig. 7, it is observed that the fracture toughness parameter decreases with  $a_o/W$  ratio.

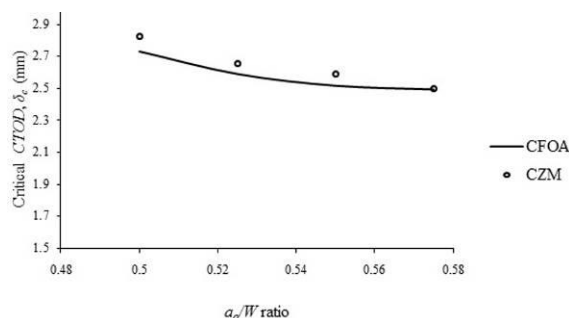


**Fig. 7: Variation of critical CTOD with  $a_o/W$  ratio**

Fracture toughness parameters for the short crack specimens ( $a/W = 0.15$  to  $0.20$ ) were found 2-3 times greater than the deep crack specimens ( $a/W = 0.50$ ) in linear elastic fracture mechanics (LEFM) regime [26-29]. According to them, shallow cracked specimens showed lower values of hydrostatic stress when compared with the deeply cracked specimens. Hydrostatic stress raises the crack tip constraint, which lowers the fracture toughness. Similarly in elastic plastic fracture mechanics (EPFM) regime, greater values of crack opening displacement (COD) and J-integral were observed in shallow cracked specimens when compared to deeply cracked specimens [29-39]. Shallow cracked specimen showed considerable crack-tip blunting and larger plastic zone in the vicinity of crack tip than deeply cracked specimens. In literature, the studies on  $a_o/W$  ratios revealed significant difference in fracture toughness for small and large  $a_o/W$  ratios. For the present work four different  $a_o/W$  ratios (0.5, 0.525, 0.55 & 0.575) are considered.

Although the chosen  $a_o/W$  ratios do not indicate any shallow crack, qualitatively comments are made on shallow cracks in conclusion section. EDD steel falls in general yield regime [6,8,10]. As plastic zone forms at the vicinity of crack tip in general yielding, plastic hinge often develops prior to failure. As  $a_o/W$  ratio increases the location of plastic hinge shifts towards the crack tip (Table 5). As hinge points shifts towards crack tip, the size of tensile plastic zone is reduced which decreases fracture toughness on increasing values of  $a_o/W$  ratio (Fig. 7). For lower values of  $a_o/W$  ratio, the drop in fracture toughness is greater but at higher values of  $a_o/W$  ratio the drop in fracture toughness reduced (Fig. 7). The decrease in fracture toughness for  $a_o/W$  ratio values, 0.5 to 0.525 is more than 5%; however the drop in fracture toughness for  $a_o/W$  ratio values, 0.55 to 0.575 is just 0.95%. Further if we increase the  $a_o/W$  ratio, fracture toughness would become independent of  $a_o/W$  ratio however this is qualitative comment.

**Table 5: Variation of location of plastic hinge with  $a_o/W$  ratio**

$a_o/W$ ratio	Plastic hinge from crack tip (mm)
0.5	11.62278
0.525	10.94527
0.55	10.28002
0.575	9.626676

### 6. Conclusion

The effect of  $a_o/W$  ratio on fracture toughness of EDD steel sheets is studied. Cohesive zone model is found suitable to characterize the EDD steel sheets. The results from proposed constant traction separation law are found to be close with the experimental findings. Similar to EPFM, in general yielding, plastic zone forms at the vicinity of crack tip and plastic hinge often develops prior to failure. It has been observed that as  $a_o/W$  ratio increases the location of plastic hinge shifts towards the crack tip (i.e. size of tensile plastic zone reduces), which reduces fracture toughness. Deeply cracked specimens would have high plastic constraint and stress at vicinity of crack than shallow cracked specimens for same crack opening displacement. Therefore the critical CTOD values decreases with increasing  $a_o/W$  ratio.

**ACKNOWLEDGEMENTS:**

The authors greatly acknowledge Product Research Group, Tata Iron and Steel Co. Ltd (TISCO) for providing enough EDD sample sheets for the present study.

**REFERENCES:**

- [1] P.J. Sun, G.J. Wang, F.Z. Xuan, S.T. Tu and Z.D. Wang. 2011. Quantitative characterization of creep constraint induced by crack depths in compact tension specimens, *Engg. Fracture Mechanics*, 78(4), 653-665. <http://dx.doi.org/10.1016/j.engfracmech.2010.11.017>.
- [2] G.Z. Wang, X.L. Liu, F.Z. Xuan and S.T. Tu. 2010. Effect of constraint induced by crack depth on creep crack-tip stress field in CT specimens, *Int. J. Solids & Structures*, 47(1), 51-57. <http://dx.doi.org/10.1016/j.ijsolstr.2009.09.015>.
- [3] C.M. Holtam, D.P. Baxter, I.A. Ashcroft and R.C. Thomson. 2010. Effect of crack depth on fatigue crack growth rates for a C-Mn pipeline steel in a sour environment, *Int. J. Fatigue*, 32(2), 288-296. <http://dx.doi.org/10.1016/j.ijfatigue.2009.06.013>.
- [4] Z.A. Chen, Z. Zeng and Y.J. Chao. 2007. Effect of crack depth on the shift of the ductile-brittle transition curve of steels, *Engg. Fracture Mechanics*, 74(15), 2437-2448. <http://dx.doi.org/10.1016/j.engfracmech.2006.11.010>.
- [5] P.J. Budden and D.W. Dean. 2007. Constraint effects on creep crack growth, *Proc. 8<sup>th</sup> Int. Conf. Creep and Fatigue at Elevated Temperatures*, San Antonio, Texas.
- [6] D.M. Kulkarni, V. Chaudhari, R. Prakash and A.N. Kumar. 2008. Effect of thickness on fracture criterion in general yielding fracture mechanics, *Int. J. Fracture*, 151, 187-198. <http://dx.doi.org/10.1007/s10704-008-9253-z>.
- [7] V.V. Chaudhari and D.M. Kulkarni. 2015. Influence of loading rate on fracture behaviour of extra deep drawn steel sheets, *Fatigue Fracture Engg. Material Structure*, 38(7), 851-859. <http://dx.doi.org/10.1111/ffe.12268>.
- [8] V.V. Chaudhari, D.M. Kulkarni and R. Prakash. 2011. Determination of critical CTOD using crack flank opening angle method in general yield regime, *Fatigue Fracture Engg. Material Structure*, 34(4), 260-269. <http://dx.doi.org/10.1111/j.1460-2695.2010.01515.x>.
- [9] V.V. Chaudhari, D.M. Kulkarni, and R. Prakash. 2010. Three-dimensional finite element analysis of fracture behavior in general yielding fracture mechanics, *J. Mechanical Engg.*, 61(3), 131-148.
- [10] V.V. Chaudhari, D.M. Kulkarni and R. Prakash. 2009. Study of influence of notch root radius on fracture behaviour of extra deep drawn steel sheets, *Fatigue Fract. Engg. Mater. Struct.*, 32(12), 975-986. <http://dx.doi.org/10.1111/j.1460-2695.2009.01401.x>.
- [11] X.P. Xu and A. Needleman. 1994. Numerical Simulations of Fast Crack Growth in Brittle Solids, *J. Mechanics and Physics of Solids*, 42(9), 1397-1434. [http://dx.doi.org/10.1016/0022-5096\(94\)90003-5](http://dx.doi.org/10.1016/0022-5096(94)90003-5).
- [12] M. Ortiz and A. Pandolfi. 1999. Finite-deformation irreversible cohesive elements for three-dimensional crack propagation analysis, *Int. J. Numerical Methods Engg.*, 44(9), 1267-1282. [http://dx.doi.org/10.1002/\(SICI\)1097-0207\(19990330\)44:9<1267::AID-NME486>3.0.CO;2-7](http://dx.doi.org/10.1002/(SICI)1097-0207(19990330)44:9<1267::AID-NME486>3.0.CO;2-7).
- [13] Y. Roy and R.H. Dodds. 2001. Simulation of ductile crack growth in thin aluminum panels using 3d surface cohesive elements, *Int. J. Fracture*, 110(1), 21-45. <http://dx.doi.org/10.1023/A:1010816201891>.
- [14] I. Scheider and W. Brocks. 2003. Simulation of cup-cone fracture using the cohesive model, *Engg. Fracture Mechanics*, 70(14), 1943-1961. [http://dx.doi.org/10.1016/S0013-7944\(03\)00133-4](http://dx.doi.org/10.1016/S0013-7944(03)00133-4).
- [15] Y. Qiu, M.A. Crisfield and G. Alfano. 2001. An interface element formulation for the simulation of delamination with buckling, *Engg. Fracture Mechanics*, 68(16), 1755-1776. [http://dx.doi.org/10.1016/S0013-7944\(01\)00052-2](http://dx.doi.org/10.1016/S0013-7944(01)00052-2).
- [16] B. Blackman, A.J. Kinloch, M. Paraschi and W.S. Teo. 2003. Measuring mode I adhesive fracture energy, gic of structural adhesive joints: the results of an international round-robin, *Int. J. Adhesion and Adhesives*, 23(4), 293-305. [http://dx.doi.org/10.1016/S0143-7496\(03\)00047-2](http://dx.doi.org/10.1016/S0143-7496(03)00047-2).
- [17] B. Blackman, H. Hadavinia and A.J. Kinloch. 2003. The calculation of adhesive fracture energies in mode I: Revisiting the tapered double cantilever beam (TDCB) test, *Engg. Fracture Mechanics*, 70(2), 233-248. [http://dx.doi.org/10.1016/S0013-7944\(02\)00031-0](http://dx.doi.org/10.1016/S0013-7944(02)00031-0).
- [18] B. Blackman, H. Hadavinia and A.J. Kinloch. 2003. The use of a cohesive zone model to study the fracture of fiber composites and adhesively-bonded joints, *Int. J. Fracture*, 119(1), 25-46. <http://dx.doi.org/10.1023/A:1023998013255>.
- [19] A. Turon, P.P. Camanho and C.G. Dávila. 2006. A damage model for the simulation of delamination in advanced composites under variable-mode loading, *Mechanics of Materials*, 38(11), 1072-1089. <http://dx.doi.org/10.1016/j.mechmat.2005.10.003>.
- [20] M. Ortiz and S. Suresh. 1993. Statistical properties of residual stresses and intergranular fracture in ceramic materials, *J. Applied Mechanics*, 60(1), 77-84. <http://dx.doi.org/10.1115/1.2900782>.
- [21] V. Tvergaard and J.W. Hutchinson. 1992. The relation between crack growth resistance and fracture process parameters in elastic-plastic solids, *J. Mechanics and Physics of Solids*, 40(6), 1377-1397. [http://dx.doi.org/10.1016/0022-5096\(92\)90020-3](http://dx.doi.org/10.1016/0022-5096(92)90020-3).
- [22] D.N. Jadhav and S.K. Maiti. 2010. Characterization of stable crack growth through AISI 4340 steel using cohesive zone modeling and CTOD/CTOA criterion, *Nuclear Engg. Design*, 240(4), 713-721. <http://dx.doi.org/10.1016/j.nucengdes.2009.11.042>.
- [23] I. Scheider, M. Schodel, W. Brocks and W. Schonfeld. 2006. Crack propagation analyses with CTOA and cohesive model: Comparison and experimental validation, *Engg. Fracture Mechanics*, 73(2), 252-263. <http://dx.doi.org/10.1016/j.engfracmech.2005.04.005>.
- [24] I. Scheider and W. Brocks. 2003. The effect of the traction separation law on the results of cohesive zone crack propagation analyses, *Key Engg. Materials*, 251(252), 313-318. <http://dx.doi.org/10.4028/www.scientific.net/KEM.251-252.313>.
- [25] U. Zerbst, M. Heinemann, C.D. Donne and D. Steglich. 2009. Fracture and damage mechanics modelling of thin-walled structures-An overview, *Engg. Fracture Mechanics*, 76(1), 5-43. <http://dx.doi.org/10.1016/j.engfracmech.2007.10.005>.
- [26] I.D. Lewis, R.F. Smith and J.F. Knott. 1975. On the a/w ratio in plane strain fracture toughness testing, *Int. J. Fracture*, 11(1), 179-183. <http://dx.doi.org/10.1007/BF00034728>.
- [27] W. Shen. 1978. Single-point method of calculating J-integral, *J. Huazhong Eng Institute*, 2, 20-24.
- [28] Q. Li, Y. Fu and X. Xu. 2005. A review of the Effect of a/W ratio on fracture toughness: Experimental

- investigation in LEFM, *J. Marine Science and Application*, 4(2), 1-5. <http://dx.doi.org/10.1007/s11804-005-0025-0>.
- [29] W.A. Sorem, J.R. Dodds and S.T. Rolfe. 1991. Effects of crack depth on elastic-plastic fracture toughness, *Int. J. Fracture*, 47(2), 105-126. <http://dx.doi.org/10.1007/BF00032572>.
- [30] Q. Li, G. Jin and Y. Wang. 2005. A review of the effect of a/W ratio on fracture toughness Experimental investigation in EPFM, *J. Marine Science & Application*, 4(1), 1-7.
- [31] Q. Li, B.H. Qiu and X.F. Cui. 2002. Effect of plastic constraint on ductile fracture in structural steels, *Proc. IWMST02*, Tokyo, Japan.
- [32] Q. Li and D. Shi. 1991. The effect of a/W ratio and crack shape on  $J_i$  and  $\delta_i$  values in a ship plate steel, *Proc. IOPE-91*, Edinburgh, U.K.
- [33] Q. Li. 2003. The effect of plastic constraint on the initiation of ductile tears in shipbuilding structural steel, *J. Marine Sci. & Application*, 2(2), 1-4.
- [34] Q. Li, L.M. Zhou and S. Li. 1986. The effect of a/w ratio on crack initiation values of COD and J-integral, *Engg. Fracture Mechanics*, 23(5), 925-928. [http://dx.doi.org/10.1016/0013-7944\(86\)90103-7](http://dx.doi.org/10.1016/0013-7944(86)90103-7).
- [35] Q. Li 1985. A study about  $J_i$  and  $\delta_i$  in three-point bend specimens with deep and shallow notches, *Engg. Frac. Mechanics*, 22(1), 9-15. [http://dx.doi.org/10.1016/0013-7944\(85\)90155-9](http://dx.doi.org/10.1016/0013-7944(85)90155-9).
- [36] X.D. Huang. 1987. *A Study About Elastic-Plastic Fracture With Deep and Shallow Crack*, J. Harbin ship building Engineering Institute, Harbin.
- [37] B. Cotterel and Q. Li. 1985. On the effect of plastic constraint on ductile tearing in a structural steel, *Engg. Fracture Mechanics*, 21(2), 239-244. [http://dx.doi.org/10.1016/0013-7944\(85\)90013-X](http://dx.doi.org/10.1016/0013-7944(85)90013-X).
- [38] C.G. Chipperfield. 1978. Some observation on ductile crack initiation and propagation in fracture toughness specimens, *Proc. Specialist Meeting on Elasto-Plastic Fracture Mechanics*, Daresbury, U.K.
- [39] J. Lin. 1987. A general formula of J-integral calculating for both shallow and deep cracks, *J. Harbin Shipbuilding Engg. Institute*, 8, 68-73.